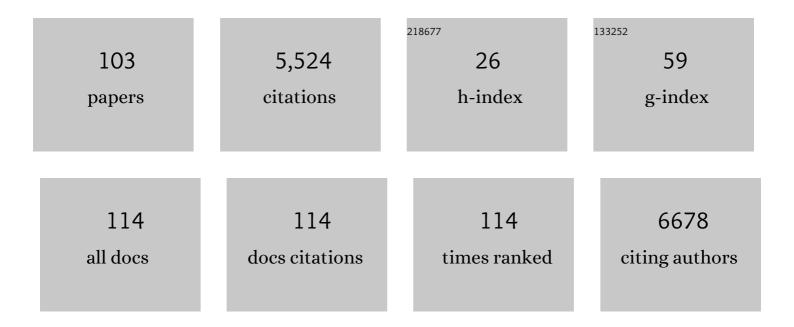
Javier Vargas

List of Publications by Year in descending order

Source: https://exaly.com/author-pdf/1206323/publications.pdf Version: 2024-02-01



LAVIED VADCAS

#	Article	IF	CITATIONS
1	The inner junction complex of the cilia is an interaction hub that involves tubulin post-translational modifications. ELife, 2020, 9, .	6.0	1,191
2	DeepEMhancer: a deep learning solution for cryo-EM volume post-processing. Communications Biology, 2021, 4, 874.	4.4	561
3	Scipion: A software framework toward integration, reproducibility and validation in 3D electron microscopy. Journal of Structural Biology, 2016, 195, 93-99.	2.8	474
4	Xmipp 3.0: An improved software suite for image processing in electron microscopy. Journal of Structural Biology, 2013, 184, 321-328.	2.8	261
5	Phase-shifting interferometry based on principal component analysis. Optics Letters, 2011, 36, 1326.	3.3	189
6	MonoRes: Automatic and Accurate Estimation of Local Resolution for Electron Microscopy Maps. Structure, 2018, 26, 337-344.e4.	3.3	179
7	Two-step demodulation based on the Gram–Schmidt orthonormalization method. Optics Letters, 2012, 37, 443.	3.3	169
8	Two-step interferometry by a regularized optical flow algorithm. Optics Letters, 2011, 36, 3485.	3.3	124
9	Asymmetric cryo-EM reconstruction of phage MS2 reveals genome structure in situ. Nature Communications, 2016, 7, 12524.	12.8	114
10	Automatic local resolution-based sharpening of cryo-EM maps. Bioinformatics, 2020, 36, 765-772.	4.1	110
11	Analysis of the principal component algorithm in phase-shifting interferometry. Optics Letters, 2011, 36, 2215.	3.3	96
12	A pattern matching approach to the automatic selection of particles from low-contrast electron micrographs. Bioinformatics, 2013, 29, 2460-2468.	4.1	73
13	Separating Actin-Dependent Chemokine Receptor Nanoclustering from Dimerization Indicates a Role for Clustering in CXCR4 Signaling and Function. Molecular Cell, 2018, 70, 106-119.e10.	9.7	70
14	Two-step self-tuning phase-shifting interferometry. Optics Express, 2011, 19, 638.	3.4	68
15	Spatial carrier phase-shifting algorithm based on principal component analysis method. Optics Express, 2012, 20, 16471.	3.4	64
16	Generalization of the Principal Component Analysis algorithm for interferometry. Optics Communications, 2013, 286, 130-134.	2.1	63
17	Efficient initial volume determination from electron microscopy images of single particles. Bioinformatics, 2014, 30, 2891-2898.	4.1	63
18	Tubulin lattice in cilia is in a stressed form regulated by microtubule inner proteins. Proceedings of the United States of America, 2019, 116, 19930-19938.	7.1	61

#	Article	IF	CITATIONS
19	Alignment of direct detection device micrographs using a robust Optical Flow approach. Journal of Structural Biology, 2015, 189, 163-176.	2.8	59
20	Fast two-dimensional simultaneous phase unwrapping and low-pass filtering. Optics Express, 2012, 20, 2556.	3.4	55
21	Survey of the analysis of continuous conformational variability of biological macromolecules by electron microscopy. Acta Crystallographica Section F, Structural Biology Communications, 2019, 75, 19-32.	0.8	49
22	Fast and accurate conversion of atomic models into electron density maps. AIMS Biophysics, 2015, 2, 8-20.	0.6	42
23	Quadrature Component Analysis for interferometry. Optics and Lasers in Engineering, 2013, 51, 637-641.	3.8	40
24	Deflectometric method for the measurement of user power for ophthalmic lenses. Applied Optics, 2010, 49, 5125.	2.1	38
25	2D simultaneous phase unwrapping and filtering: A review and comparison. Optics and Lasers in Engineering, 2012, 50, 1026-1029.	3.8	38
26	Local computational methods to improve the interpretability and analysis of cryo-EM maps. Nature Communications, 2021, 12, 1240.	12.8	36
27	CTF Challenge: Result summary. Journal of Structural Biology, 2015, 190, 348-359.	2.8	34
28	Role of Era in assembly and homeostasis of the ribosomal small subunit. Nucleic Acids Research, 2019, 47, 8301-8317.	14.5	34
29	FASTDEF: Fast defocus and astigmatism estimation for high-throughput transmission electron microscopy. Journal of Structural Biology, 2013, 181, 136-148.	2.8	31
30	Particle quality assessment and sorting for automatic and semiautomatic particle-picking techniques. Journal of Structural Biology, 2013, 183, 342-353.	2.8	31
31	Pea PSII-LHCII supercomplexes form pairs by making connections across the stromal gap. Scientific Reports, 2017, 7, 10067.	3.3	30
32	A review of resolution measures and related aspects in 3D Electron Microscopy. Progress in Biophysics and Molecular Biology, 2017, 124, 1-30.	2.9	30
33	A Survey of the Use of Iterative Reconstruction Algorithms in Electron Microscopy. BioMed Research International, 2017, 2017, 1-17.	1.9	29
34	A new algorithm for high-resolution reconstruction of single particles by electron microscopy. Journal of Structural Biology, 2018, 204, 329-337.	2.8	28
35	Measuring local-directional resolution and local anisotropy in cryo-EM maps. Nature Communications, 2020, 11, 55.	12.8	28
36	A statistical approach to the initial volume problem in Single Particle Analysis by Electron Microscopy. Journal of Structural Biology, 2015, 189, 213-219.	2.8	27

#	Article	IF	CITATIONS
37	Single-particle electron microscopy structure of UDP-glucose:glycoprotein glucosyltransferase suggests a selectivity mechanism for misfolded proteins. Journal of Biological Chemistry, 2017, 292, 11499-11507.	3.4	26
38	Flexible calibration procedure for fringe projection profilometry. Optical Engineering, 2007, 46, 023601.	1.0	25
39	Fringe pattern denoising by image dimensionality reduction. Optics and Lasers in Engineering, 2013, 51, 921-928.	3.8	25
40	Semiautomatic, High-Throughput, High-Resolution Protocol for Three-Dimensional Reconstruction of Single Particles in Electron Microscopy. Methods in Molecular Biology, 2013, 950, 171-193.	0.9	25
41	A fast iterative convolution weighting approach for gridding-based direct Fourier three-dimensional reconstruction with correction for the contrast transfer function. Ultramicroscopy, 2015, 157, 79-87.	1.9	25
42	Deep Learning for Validating and Estimating Resolution of Cryo-Electron Microscopy Density Maps â€. Molecules, 2019, 24, 1181.	3.8	25
43	Phase-shifting interferometry based on induced vibrations. Optics Express, 2011, 19, 584.	3.4	24
44	Principal component analysis based simultaneous dual-wavelength phase-shifting interferometry. Optics Communications, 2015, 341, 276-283.	2.1	24
45	XTEND: Extending the depth of field in cryo soft X-ray tomography. Scientific Reports, 2017, 7, 45808.	3.3	24
46	High strength brushite bioceramics obtained by selective regulation of crystal growth with chiral biomolecules. Acta Biomaterialia, 2020, 106, 351-359.	8.3	24
47	Phase-shifting VU factorization for interferometry. Optics and Lasers in Engineering, 2020, 124, 105797.	3.8	22
48	Advances in Xmipp for Cryo–Electron Microscopy: From Xmipp to Scipion. Molecules, 2021, 26, 6224.	3.8	22
49	Imaging polarimeters based on liquid crystal variable retarders: an emergent technology for space instrumentation. Proceedings of SPIE, 2011, , .	0.8	21
50	Particle alignment reliability in single particle electron cryomicroscopy: a general approach. Scientific Reports, 2016, 6, 21626.	3.3	21
51	Alternative conformations and motions adopted by 30S ribosomal subunits visualized by cryo-electron microscopy. Rna, 2020, 26, 2017-2030.	3.5	21
52	Optical inspection of liquid crystal variable retarder inhomogeneities. Applied Optics, 2010, 49, 568.	2.1	20
53	Shack–Hartmann centroid detection method based on high dynamic range imaging and normalization techniques. Applied Optics, 2010, 49, 2409.	2.1	20
54	Non-uniformly polarized beams across their transverse profiles: an introductory study for undergraduate optics courses. European Journal of Physics, 2004, 25, 793-800.	0.6	19

#	Article	IF	CITATIONS
55	Three-dimensional reconstruction methods in Single Particle Analysis from transmission electron microscopy data. Archives of Biochemistry and Biophysics, 2015, 581, 39-48.	3.0	19
56	Scipion web tools: Easy to use cryoâ€EM image processing over the web. Protein Science, 2018, 27, 269-275.	7.6	18
57	Shack–Hartmann centroid detection using the spiral phase transform. Applied Optics, 2012, 51, 7362.	1.8	17
58	Circular common-path point diffraction interferometer. Optics Letters, 2012, 37, 3927.	3.3	16
59	Error analysis of the principal component analysis demodulation algorithm. Applied Physics B: Lasers and Optics, 2014, 115, 355-364.	2.2	16
60	Cryo-EM and the elucidation of new macromolecular structures: Random Conical Tilt revisited. Scientific Reports, 2015, 5, 14290.	3.3	16
61	Quantitative interferometric microscopy cytometer based on regularized optical flow algorithm. Optics Communications, 2015, 350, 222-229.	2.1	16
62	Denoising of high-resolution single-particle electron-microscopy density maps by their approximation using three-dimensional Gaussian functions. Journal of Structural Biology, 2016, 194, 423-433.	2.8	16
63	Shack-Hartmann spot dislocation map determination using an optical flow method. Optics Express, 2014, 22, 1319.	3.4	15
64	Quantitative analysis of 3D alignment quality: its impact on soft-validation, particle pruning and homogeneity analysis. Scientific Reports, 2017, 7, 6307.	3.3	15
65	Local fringe density determination by adaptive filtering. Optics Letters, 2011, 36, 70.	3.3	14
66	High dynamic range imaging method for interferometry. Optics Communications, 2011, 284, 4141-4145.	2.1	13
67	Windowed phase unwrapping using a first-order dynamic system following iso-phase contours. Applied Optics, 2012, 51, 7549.	1.8	13
68	Comparing scientific performance among equals. Scientometrics, 2014, 101, 1731-1745.	3.0	12
69	Multivalent interactions essential for lentiviral integrase function. Nature Communications, 2022, 13, 2416.	12.8	12
70	Calibration of a Shack–Hartmann wavefront sensor as an orthographic camera. Optics Letters, 2010, 35, 1762.	3.3	11
71	Principal component analysis-based quantitative differential interference contrast microscopy. Optics Letters, 2019, 44, 45.	3.3	11
72	A robust approach to ab initio cryo-electron microscopy initial volume determination. Journal of Structural Biology, 2019, 208, 107397.	2.8	10

#	Article	IF	CITATIONS
73	Novel multiresolution approach for an adaptive structured light system. Optical Engineering, 2008, 47, 023601.	1.0	9
74	Local analysis of strains and rotations for macromolecular electron microscopy maps. Journal of Structural Biology, 2016, 195, 123-128.	2.8	9
75	Three-dimensional measurement of microchips using structured light techniques. Optical Engineering, 2008, 47, 053602.	1.0	8
76	Space-qualified liquid-crystal variable retarders for wide-field-of-view coronagraphs. , 2011, , .		8
77	Multiplicative phase-shifting interferometry using optical flow. Applied Optics, 2012, 51, 5903.	1.8	8
78	Precise phase retrieval under harsh conditions by constructing new connected interferograms. Scientific Reports, 2016, 6, 24416.	3.3	8
79	Interchanging Geometry Conventions in 3DEM: Mathematical Context for the Development of Standards. Applied and Numerical Harmonic Analysis, 2014, , 7-42.	0.3	8
80	Effect of Aberrations on the Self-Imaging Phenomenon. Journal of Lightwave Technology, 2011, 29, 1051-1057.	4.6	7
81	Blind estimation of DED camera gain in Electron Microscopy. Journal of Structural Biology, 2018, 203, 90-93.	2.8	7
82	Adaptive spatiotemporal structured light method for fast three-dimensional measurement. Optical Engineering, 2006, 45, 107203.	1.0	6
83	Direct demodulation of closed-fringe interferograms based on active contours. Optics Letters, 2010, 35, 3550.	3.3	6
84	Robust weighted principal components analysis demodulation algorithm for phase-shifting interferometry. Optics Express, 2021, 29, 16534.	3.4	6
85	On the development of three new tools for organizing and sharing information in three-dimensional electron microscopy. Acta Crystallographica Section D: Biological Crystallography, 2013, 69, 695-700.	2.5	5
86	Fast and automatic identification of particle tilt pairs based on Delaunay triangulation. Journal of Structural Biology, 2016, 196, 525-533.	2.8	4
87	Foil-hole and data image quality assessment in 3DEM: Towards high-throughput image acquisition in the electron microscope. Journal of Structural Biology, 2016, 196, 515-524.	2.8	4
88	Enhancement of Cryo-EM maps by a multiscale tubular filter. Optics Express, 2022, 30, 4515.	3.4	4
89	Incremental PCA algorithm for fringe pattern demodulation. Optics Express, 2022, 30, 12278.	3.4	4
90	Multiresolution approach based on projection matrices. Applied Optics, 2009, 48, 1295.	2.1	3

#	Article	IF	CITATIONS
91	Regularized least squares phase sampling interferometry. Optics Express, 2011, 19, 5002.	3.4	3
92	Rapid quantitative interferometric microscopy using fast Fourier transform and differential–integral based phase retrieval algorithm (FFT-DI-PRA). Optics Communications, 2020, 456, 124613.	2.1	3
93	Role of the filter phase in phase sampling interferometry. Optics Express, 2011, 19, 19987.	3.4	2
94	Digital image compression for a 2f multiplexing optical setup. Journal of Optics (United Kingdom), 2016, 18, 075701.	2.2	2
95	ENRICH: A fast method to improve the quality of flexible macromolecular reconstructions. Progress in Biophysics and Molecular Biology, 2021, 164, 92-100.	2.9	2
96	A two steps phase-shifting demodulation method using the VU factorization. Optics and Lasers in Engineering, 2021, 147, 106730.	3.8	2
97	Defect inspection by an active 3D multiresolution technique. , 2008, , .		1
98	Facial morphology analysis in osteogenesis imperfecta types I, III and IV using computer vision. Orthodontics and Craniofacial Research, 2021, 24, 92-99.	2.8	1
99	A comprehensive review of the principal component analysis applied to the demodulation of phase-shifting interferograms. , 2020, , .		1
100	An image processing approach to the simulation of electron microscopy volumes of atomic structures. , 2014, , .		0
101	Computational Methods to Process Highly Heterogeneous Cryo-EM Samples. Microscopy and Microanalysis, 2019, 25, 1292-1293.	0.4	0
102	Improving 3D reconstructions of macromolecular conformations. Acta Crystallographica Section A: Foundations and Advances, 2018, 74, a155-a155.	0.1	0
103	Linear algebra approach to phase shifting interferometry: numerical methods. , 2019, , .		0